

Vipin Kumar Marina L. Gavrilova  
Chih Jeng Kenneth Tan Pierre L'Ecuyer (Eds.)

# Computational Science and Its Applications – ICCSA 2003

International Conference  
Montreal, Canada, May 18-21, 2003  
Proceedings, Part II



Springer

991) 257  
is of wave propagation using  
.993) 207–227  
ctral finite element model for  
ation in laminated composite

of nonlinear interactions. Me-  
) 711–727  
ures. Appl. Mech. Rev. **52**(2)

s of the complex wave spec-  
medium. Part I. Theory and  
) (1997) 896–920

ave approach to estimating  
ng. J. Sound and Vibration,

two-dimensional focusing and  
a. Soviet Physics, JETP, **34**

es. Johns Hopkins University

er-Verlag, 1997  
ral finite element for analysis  
of Sound and Vibration (in

# Finite Element Analysis of Nanowire Superlattice Structures

M. Willatzen<sup>1</sup>, R.V.N. Melnik<sup>1</sup>, C. Galeriu<sup>2</sup>, and L.C. Lew Yan Voon<sup>2</sup>

<sup>1</sup> University of Southern Denmark,  
Mads Clausen Institute, DK-6400, Denmark

<sup>2</sup> Worcester Polytechnic Institute,  
Department of Physics, MA 01609, USA

**Abstract.** Finite Element calculations were performed on finite nanowire superlattice (NWSL) structures with a cylindrical cross section so as to determine electronic eigenstates and energy eigenvalues. In recent years, such structures have been grown as they are good candidates for use in active regions of future optoelectronic devices. In particular, we analyzed the qualitative differences in terms of wavefunctions and energy eigenvalues between structures containing the same number of barriers and wells (asymmetrical) and structures where the number of barrier layers is one above the number of well layers (symmetrical). Dirichlet boundary conditions were imposed on the surface of the nanowire structures corresponding to the case where the nanostructure environment is vacuum. We compared our results with those available for the Kronig-Penney model describing infinite NWSLs. Asymmetrical NWSL structures show qualitative and quantitative differences as compared to both symmetrical NWSL structures and infinite periodic NWSL structures.

## 1 Introduction

Nanowire superlattice structures are new exciting nanostructures which can be grown using various growth techniques. In this way, longitudinally modulated nanowires can be grown [1,2,3] with nanowire radii of 200–400 Å and layer width of 150–1000 Å. NWSL structures are expected to find applications as nanobar codes, waveguides, lasers, and light-emitting diodes. In particular, it has been argued that NWSL structures possibly show better characteristic properties as compared to plain nanowires [4] due to the coupling of superlattice longitudinal confinement to the nanowire radial confinement. These characteristic properties include the extremely polarized photoluminescence of a NWSL and the non-ohmic conductance of a NWSL with a single barrier.

In the present work, the finite nanowire superlattice problem was examined using a one-band model for electrons in the conduction band. Thus, the approach taken here is expected to give accurate results for the GaAs/Al<sub>0.3</sub>Ga<sub>0.7</sub>As nanostructures where non-parabolicity effects are of minor importance due to the large bandgap present. We employed the Finite Element Method (FEM) so as to calculate electron eigenvalues and eigenstates for a series of finite NWSL structures

with a cylindrical cross-section. The NWSL structures considered are symmetrical or asymmetrical (with respect to a center plane of the nanostructure) in the following sense. For the symmetrical structures, we assumed  $N + 1$  layers in the NWSL structure are barrier layers. Then,  $N$  layers are well layers where  $N$  is an integer (see Figure 1). Similarly, for the asymmetrical structure, we assumed  $N$  layers in the NWSL structure are barrier layers, then  $N$  layers are well layers where  $N$  is an integer. The former structures are symmetrical because a mirror reflection around the center plane of the structure leaves the structure unchanged while this is not the case for the latter (asymmetrical) structures.

We discuss the wavefunction properties of the various NWSL structures and show that the eigenvalues found for a finite symmetrical structure converges towards the Kronig-Penney model results for eigenvalues if the number of wells increases towards infinity. Moreover, we also found that the energy spectrum for finite NWSL symmetrical structures with the number of unit cells above 6–7 is similar to the energy spectrum found in the Kronig-Penney model case. There are qualitative and quantitative differences when considering asymmetrical NWSL structures with a barrier layer at one end and a well layer at the other end as compared to symmetrical finite NWSL structures and the infinite periodic (Kronig-Penney) NWSL structure.

## 2 Theory

The nanowire superlattice was modeled as an ideal cylinder with sharp modulations in the longitudinal (or  $z$  direction) (Figure 1). The electronic structure is given by solving the Ben Daniel-Duke equation [5]:

$$-\frac{\hbar^2}{2} \nabla \cdot \left[ \frac{1}{m(\mathbf{r})} \nabla \psi(\mathbf{r}) \right] + V(\mathbf{r})\psi(\mathbf{r}) = E\psi(\mathbf{r}), \quad (1)$$

where  $V(\mathbf{r})$  is the potential experienced by the electron [will be taken to be infinite outside the wire (vacuum) and piecewise constant inside],  $m(\mathbf{r})$  is the effective mass in each superlattice layer,  $\psi$  is the wave function, and  $E$  is the energy. As mentioned above, nonparabolicity effects were neglected which is a good approximation for large bandgap materials such as  $\text{Al}_{0.3}\text{Ga}_{0.7}\text{As}/\text{GaAs}$ . Because the potential and the effective mass are functions of the axial coordinate  $z$  only, the partial differential equation is separable in all three cylindrical circular coordinates, leading to the following set of ordinary differential equations:

$$\begin{aligned} \frac{d^2\Phi(\phi)}{d\phi^2} + l^2\Phi(\phi) &= 0, \\ r \frac{d}{dr} \left( r \frac{dJ}{dr} \right) + [q^2r^2 - l^2] J(r) &= 0, \\ \frac{d}{dz} \left( \frac{1}{m(z)} \frac{dZ(z)}{dz} \right) + \frac{2}{\hbar^2} \left[ E - V(z) - \frac{\hbar^2 q^2}{2m(z)} \right] Z(z) &= 0, \end{aligned} \quad (2)$$

considered are symmetries of the nanostructure) in assumed  $N + 1$  layers are well layers where electrical structure, we assume, then  $N$  layers are well symmetrical because a single layer leaves the structure unimmetrical structures. In NWSL structures and the structure converges if the number of wells in the energy spectrum for unit cells above 6–7 is the model case. There are two asymmetrical NWSL layers at the other end and the infinite periodic

order with sharp modulations in the electronic structure

$$\nabla \psi(\mathbf{r}), \quad (1)$$

will be taken to be zero inside],  $m(\mathbf{r})$  is the mass function, and  $E$  is the energy neglected which is as  $\text{Al}_{0.3}\text{Ga}_{0.7}\text{As}/\text{GaAs}$ . of the axial coordinate three cylindrical circular differential equations:

$$\nabla^2 \Phi(\phi) = 0,$$

$$\nabla J(r) = 0, \quad (2)$$

$$\nabla Z(z) = 0,$$

where we have written  $\psi(r, \phi, z) = J(r)\Phi(\phi)Z(z)$ . The solution to the first of Equation (2) — the angular equation — is trivial,  $\Phi(\phi) = e^{il\phi}$ , with  $l$  an integer. The solution to the second of Equation (2) — the radial equation — is a Bessel function of the first kind, with the wave number  $q$  determined by the boundary condition  $J_l(qR) = 0$ , where  $R$  is the radius of the NWSL. The third equation of Equation (2) is the longitudinal equation.

Note, as a more general case, that when the potential  $V$  and/or the effective mass  $m$  is a function of both  $z$  and  $r$ , the general 3D problem [Equation (1)] can be separated in the azimuthal coordinate  $\phi$  only, and we obtain

$$-\frac{\hbar^2}{2} \frac{\partial}{\partial z} \left( \frac{1}{m(z, r)} \frac{\partial \chi_l}{\partial z} \right) - \frac{\hbar^2}{2} \frac{1}{r} \frac{\partial}{\partial r} \left( \frac{r}{m(z, r)} \frac{\partial \chi_l}{\partial r} \right) + \frac{\hbar^2}{2m(z, r)} \frac{l^2}{r^2} \chi_l(z, r) + V(z, r) \chi_l(z, r) = E \chi_l(z, r), \quad (3)$$

with  $\psi(r, \phi, z) = \chi_l(z, r) \exp(il\phi)$ . This particular case is of physical relevance when, e.g., the NWSL structure is embedded in a material different from vacuum. In actual fact, we solved the more general mathematical problem [Equation (3)] using the FEM for all examples discussed in the present work.

### 3 Numerical Technique for Eigenvalue PDE Problems of Ben Daniel-Duke Type

Problem (3) is supplemented by appropriate boundary conditions, and is cast in the variational form. The finite element discretisation was applied to project that form onto a finite-dimensional space, and all integrals were approximated with Gaussian quadratures. As a result, the problem was reduced to the following generalised eigenvalue problem:

$$A\mathbf{u} = \lambda B\mathbf{u}, \quad (4)$$

where matrices  $A$  and  $B$  are  $N \times N$  matrices,  $\mathbf{u}$  is the vector of unknowns of dimensionality  $N$ , and  $N$  is the number of nodes in which the solution to the problem (3) is being sought. Computational domains of interest are symmetric with respect to the  $z$ -axis, where we imposed Neumann's boundary conditions if  $l = 0$ , and Dirichlet's boundary conditions otherwise. The rest of the structures are bordered with vacuum, and hence Dirichlet's boundary conditions were imposed in that case. In computations that we have performed so far, the number of elements varied from around 5,000 up to 200,000 and the number of nodes varied from several thousands to around 150,000, depending on the size of the structure and the required accuracy. The solution to Equation (4) was found in an iterative manner by using the Krylov subspace projective methodology. We have used an orthogonal projection (e.g., [6]); in particular, the core of the solver is the spectral Arnoldi iteration method.

We searched for all eigenvalues of the problem in the given interval. The boundary estimates for the interval follows directly from the physics of the

problem, and in the case analysed here they are 0 eV for the lower bound (the GaAs conduction band edge) and 0.23 eV for the upper bound (the  $\text{Al}_{0.3}\text{Ga}_{0.7}\text{As}$  potential barrier). The procedure was easily implemented in the Matlab-based Femlab environment (e.g., [7]). Adaptive mesh refinements were used to ensure convergence on a sequence of grids.

#### 4 Results and Discussions

In the following, we discuss only states with azimuthal symmetry, i.e., states for which  $l = 0$ . It must be emphasized, however, that states with  $l \neq 0$  can be found in a completely analogous manner — without any problems — using the procedure described in Section 3. Our discussion that follows is based on the NWSL structures that consist of 50 Å GaAs well layers ( $L_w$  in Figure 1) and 50 Å  $\text{Al}_{0.3}\text{Ga}_{0.7}\text{As}$  barrier layers ( $L_b$  in Figure 1) stacked in an alternate fashion. The radius,  $R$ , is 100 Å for all layers, i.e., 100 Å for the whole NWSL layer (Figure 1).

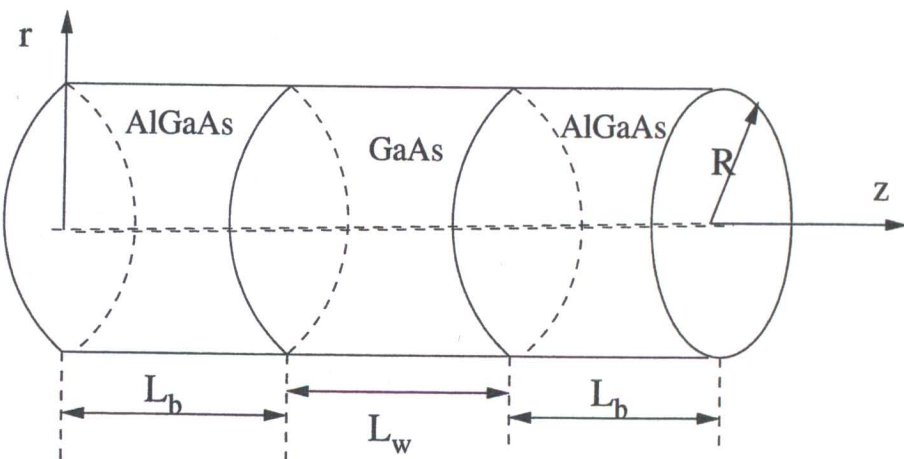
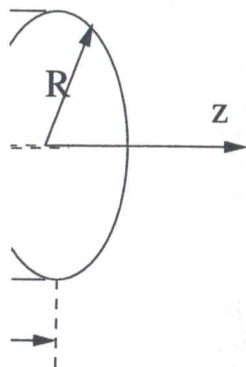


**Fig. 1.** Schematic representation of nanowire geometry

In Figure 2, we show the two bound states found for the asymmetrical structure with two well layers. These states have energies 0.1046 eV and 0.1489 eV, respectively, and both states have zero nodes along the radial direction. Since the mirror reflection operator about the center plane is not a symmetry for the asymmetrical structure, neither the ground state nor the first excited state will be symmetric (or antisymmetric) with respect to the same center plane. This is

the lower bound (the bound (the  $\text{Al}_{0.3}\text{Ga}_{0.7}\text{As}$  d in the Matlab-based ts were used to ensure

symmetry, i.e., states states with  $l \neq 0$  can any problems — using at follows is based on years ( $L_w$  in Figure 1) stacked in an alternate for the whole NWSL



geometry

e asymmetrical struc-  
46 eV and 0.1489 eV,  
adial direction. Since  
t a symmetry for the  
irst excited state will  
center plane. This is

clearly observed in Figure 2. The reason behind the rather large energy difference between the two states is the following. The ground state is predominantly located in the GaAs well layer sandwiched between two  $\text{Al}_{0.3}\text{Ga}_{0.7}\text{As}$  barrier layers (with potential barriers of 0.23 eV) while the excited state is predominantly located in the GaAs well layer sandwiched by a  $\text{Al}_{0.3}\text{Ga}_{0.7}\text{As}$  barrier layer and vacuum (with potentials 0.23 eV and  $\infty$ , respectively).

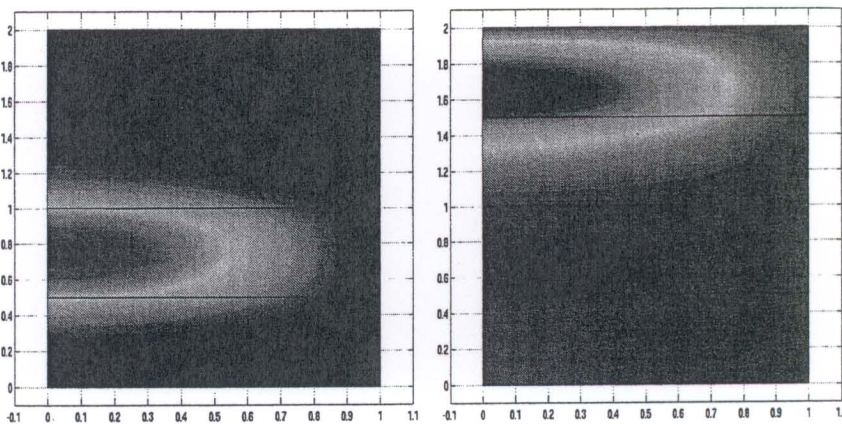
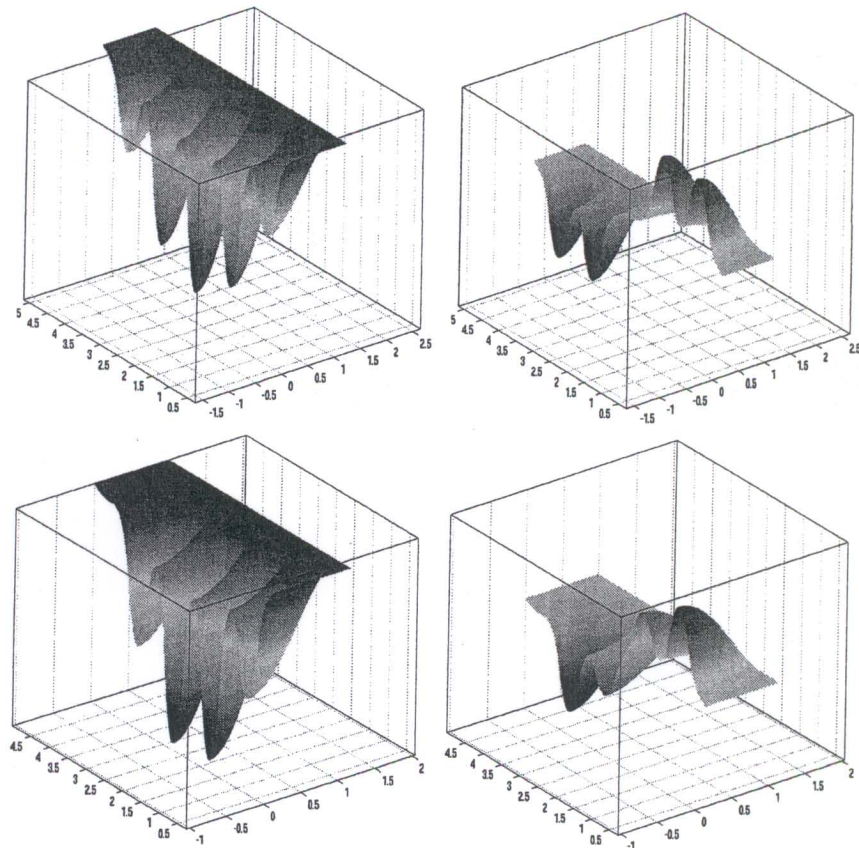


Fig. 2. Asymmetric nanowire with 2 wells: ground and first excited states

In Figure 3, we compare numerical results for the ground state and the first excited state of (a) the symmetrical structure consisting of five well layers and six barrier layers, and (b) the asymmetrical structure consisting of five well layers and five barrier layers. It is evident that the ground state (first excited state) of the former structure is symmetric (antisymmetric) with respect to a mirror reflection in the center plane of the NWSL structure due to the fact that the mirror reflection operator is a symmetry for the symmetrical structure. As mentioned above, no such mirror reflection symmetry exists for the asymmetrical structure and therefore the ground state (first excited state) is also not symmetric (antisymmetric) with respect to a mirror reflection in the center plane. It follows by inspection of the various eigenmodes and eigenvalues for the asymmetrical structure that three eigenstates have almost the same energy as the ground state — all of them between 0.10 and 0.11 eV above the conduction-band edge of GaAs (in the following energies are calculated with the GaAs conduction-band edge as a reference). This is a consequence of the fact that the symmetrical structure consists of five wells and that four of these wells are located between two barrier layers of  $\text{Al}_{0.3}\text{Ga}_{0.7}\text{As}$ . The first four states are all predominantly associated with these four wells. The remaining fifth state is, however, predominantly associated with the fifth well sandwiched between a  $\text{Al}_{0.3}\text{Ga}_{0.7}\text{As}$  barrier layer and vacuum,

and thus has a substantially higher energy (again refer to the discussion above). Returning to the symmetrical structure, note that here all five well layers are sandwiched between  $\text{Al}_{0.3}\text{Ga}_{0.7}\text{As}$  layers, hence the five states associated with the well layers must have approximately the same energy [between 0.10 and 0.11 eV].

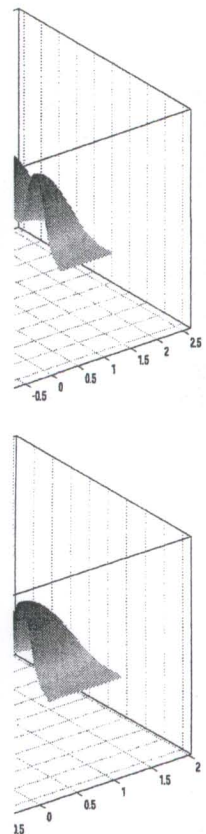


**Fig. 3.** Symmetric (top) and asymmetric nanowire with 5 wells: ground and first excited states

In Figure 4, contour plots of the ground-state envelope functions for four symmetrical structures are shown with 1, 2, 7, and 12 well layers. Our FEM calculations capture well the fact that the number of energy eigenvalues close to the ground state energy is equal to the number of well layers (in all cases with energies between 0.10 and 0.11 eV). Since  $l = 0$ , the states found with

the discussion above). all five well layers are states associated with energy [between 0.10 and

energies close to 0.10 and 0.11 eV correspond to the first zero of Bessel's function  $J_0$ , i.e.,  $q = 2.40/R$ . The eigenstates with one or more nodes along the radial direction were not found in the energy search interval  $0 - 0.23$  eV where 0.23 eV is the conduction band edge of  $\text{Al}_{0.3}\text{Ga}_{0.7}\text{As}$  reflecting the fact that such states are spread all over the NWSL structure with no exponential decay in the  $\text{Al}_{0.3}\text{Ga}_{0.7}\text{As}$  barrier regions.



wells: ground and first

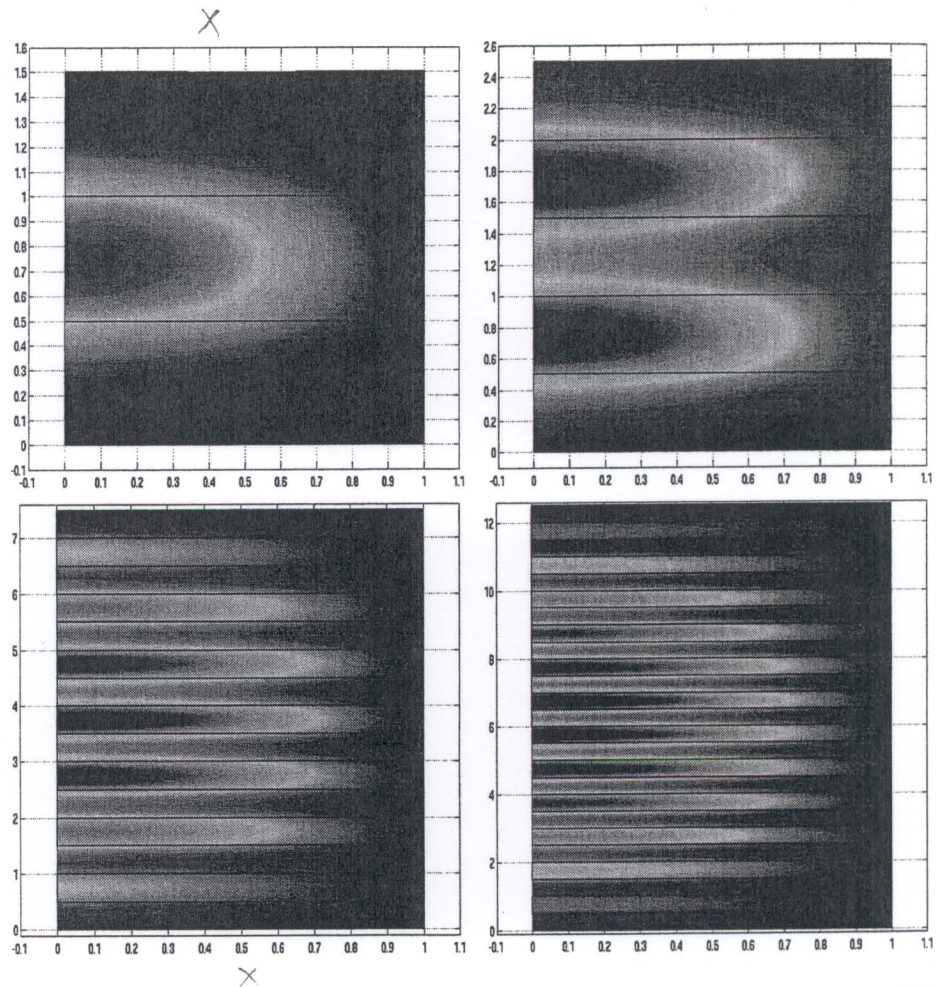
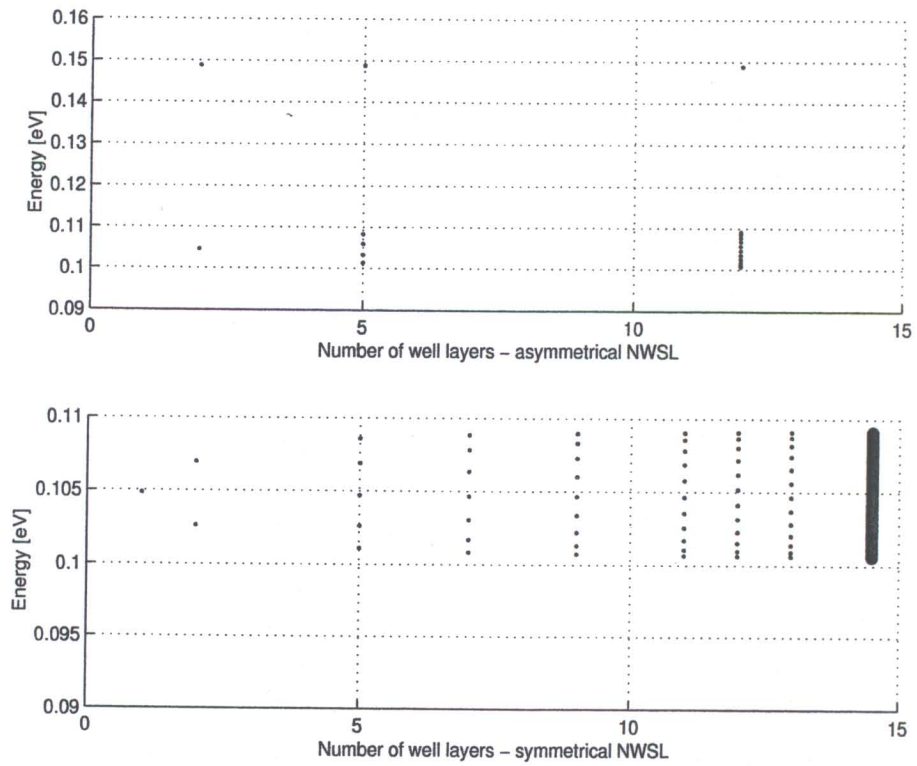


Fig. 4. Ground state in symmetric nanowires (one, two, seven and twelve wells)

ope functions for four well layers. Our FEM energy eigenvalues close well layers (in all cases the states found with

In Figure 5, we plot energy eigenvalues as a function of the number of well layers for asymmetrical (top figure) and symmetrical (lower figure) NWSL structures. The qualitative behavior discussed above for symmetrical and asymmet-

rical structures can be seen in Figure 5. Moreover, it is found that the energy eigenvalue range for the symmetrical structure approaches that of the Kronig-Penney (KP) model case (corresponding to an infinite number of unit cells where each unit cell consists of a single well layer and a single barrier layer) as  $N \rightarrow \infty$ . It is interesting to note that the state predominantly associated with the well layer sandwiched between vacuum and a  $\text{Al}_{0.3}\text{Ga}_{0.7}\text{As}$  barrier layer — found in the asymmetrical structures only — finds no analogue in any symmetrical NWSL structure or in the KP structure due to different symmetry properties.



**Fig. 5.** Comparisons with the KP model. The KP model results are shown to the far right.

## 5 Conclusions

The finite element method has been applied to examine eigenvalues and eigenfunctions of nanowire superlattice structures with a cylindrical cross-section. It

found that the energy levels of the Kronig-Penney model of unit cells where the barrier layer) as  $N \rightarrow \infty$ . Associated with the well barrier layer — found to be in any symmetrical symmetry properties.

is shown that qualitative differences exist in the electronic wavefunctions between NWSL structures consisting of (a)  $N + 1$  barrier layers and  $N$  well layers, and (b)  $N$  barrier layers and  $N$  well layers where  $N$  is an integer. In addition, we have compared eigenvalues and eigenfunctions obtained in our calculations with exact Kronig-Penney model results. Our modelling results have confirmed that finite symmetrical NWSL structures with increasing numbers of  $N$  behave like an infinite NWSL structure. However, in the case of asymmetrical finite NWSL structures, a bound state exists which finds no analogue in the symmetrical NWSL structure or in the Kronig-Penney model case corresponding to an infinite (periodic) NWSL structure.

## 6 Acknowledgments

Two of the authors, LCLYV and CG, were supported by an NSF CAREER award (NSF Grant No. 9984059).

## References

1. Gudiksen, M.S., Lauhon, L. J., Wang, J., Smith, D.C., and Lieber, C.M.: Growth of nanowire superlattice structures for nanoscale photonics and electronics. *Nature* 415 (2002) 617-620
2. Wu, Y., Fan, R., and Yang, P.: Block-by-block growth of single-crystalline Si/SiGe superlattice nanowires. *Nano Letters* 2 (2002) 83-86
3. Björk, M. T., Ohlsson, B. J., Sass, T., Persson, A. I., Thelander, C., Magnusson, M. H., Deppert, K., Wallenberg, L.R., and Samuelson, L.: One-dimensional steeplechase for electrons realized. *Nano Letters* 2 (2002) 87-89
4. Wang, J., Gudiksen, M.S., Duan, X., Cui, Y., and Lieber, C.M.: Highly polarized photoluminescence and photodetection from single indium phosphide nanowires. *Science* 293 (2001) 1455-1457
5. Bastard, G., *Wave Mechanics Applied to Semiconductor Heterostructures*. Les Editions de Physique, Les Ulis (1988)
6. Quarteroni, A., Sacco, R., and Saleri, F.: *Numerical Mathematics*. Springer-Verlag, Berlin Heidelberg New York (2000)
7. Femlab Reference Manual. Version 2.3. Comsolab (2002)

all results are shown to

eigenvalues and eigenfunctions of the cylindrical cross-section. It